

# Offline Parameter Identification and State-of-Charge Estimation for Healthy and Aged Electric Vehicle Batteries Based on the Combined Model

Xiaowei Zhang, Min Xu, Saeid Habibi, Fengjun Yan, Ryan Ahmed

**Abstract**—Recently, Electric Vehicles (EVs) have received extensive consideration since they offer a more sustainable and greener transportation alternative compared to fossil-fuel propelled vehicles. Lithium-Ion (Li-ion) batteries are increasingly being deployed in EVs because of their high energy density, high cell-level voltage, and low rate of self-discharge. Since Li-ion batteries represent the most expensive component in the EV powertrain, accurate monitoring and control strategies must be executed to ensure their prolonged lifespan. The Battery Management System (BMS) has to accurately estimate parameters such as the battery State-of-Charge (SOC), State-of-Health (SOH), and Remaining Useful Life (RUL). In order for the BMS to estimate these parameters, an accurate and control-oriented battery model has to work collaboratively with a robust state and parameter estimation strategy. Since battery physical parameters, such as the internal resistance and diffusion coefficient change depending on the battery state-of-life (SOL), the BMS has to be adaptive to accommodate for this change. In this paper, an extensive battery aging study has been conducted over 12-months period on 5.4 Ah, 3.7 V Lithium polymer cells. Instead of using fixed charging/discharging aging cycles at fixed C-rate, a set of real-world driving scenarios have been used to age the cells. The test has been interrupted every 5% capacity degradation by a set of reference performance tests to assess the battery degradation and track model parameters. As battery ages, the combined model parameters are optimized and tracked in an offline mode over the entire batteries lifespan. Based on the optimized model, a state and parameter estimation strategy based on the Extended Kalman Filter (EKF) and the relatively new Smooth Variable Structure Filter (SVSF) have been applied to estimate the SOC at various states of life.

**Keywords**—Lithium-Ion batteries, genetic algorithm optimization, battery aging test, and parameter identification.

## I. INTRODUCTION

EVs are becoming a widely used transportation mode since they offer numerous benefits such as their small environmental impact and their high well-to-wheel efficiency [1]. The battery pack is one of the most expensive components in the EV powertrain, therefore, highly accurate monitoring, control, and protection strategies have to be implemented onboard of the BMS to prolong the battery lifespan and ensure safety [2]. However, several electrification challenges, such as cost, range anxiety, safety, and reliability still hinder the wide adoption and mass market production of EVs [3]. These challenges could be significantly mitigated by incorporating

an advanced BMS. The BMS represents the brain of the battery; it is responsible for monitoring the battery SOC and SOH, and ensuring safety by safeguarding against short circuits and over-charge/under-discharge conditions. In addition, the BMS ensures cell-to-cell balancing, conducts thermal management, and estimates instantaneous available power [4]. The battery SOC is one of the key variables monitored by the BMS since it is strongly linked to the vehicle driving range which is of a great concern to the driver. Therefore, an accurate SOC estimation will ultimately improve the customer satisfaction and accelerate the mass market acceptance of EVs. The battery SOC estimation is a relatively complex task since the battery characteristics change over time; as battery ages, it exhibits capacity and power fade, and its internal resistance increases which in turn affect the model and SOC estimation accuracy. Thus, battery models have to be adaptive in order to accommodate for the changes in battery characteristics and performance across the entire battery states of life.

Recently, several incidents of battery degradation have been reported. For instance, as per October, 2012, there were 112 documented cases of customers complaining of capacity loss in EVs [5]. Manufacturers generally have lifetime data on batteries, but these are generated by using predefined charging/discharging cycles at fixed temperatures and fixed charging/discharging rates referred to as C-rate. Relying on this data in model development will result in inaccuracies and errors in SOC and SOH estimations. The EV battery is not simply like portable application whose current rate profile is piecewise constant [5]. The battery in EV applications operates in a dynamic environment with fast transients and aggressive current requirement. Accordingly, these fast transients need to be captured by the battery aging model and parameters have to be tracked accordingly.

Numerous research studies on battery aging and SOH estimation have been presented in the literature [6]-[9]. Based on a ninth-order polynomial model, Stamps et al. have implemented a hybrid estimation algorithm and discrete filtering of batch estimation to predict the capacity fade and the change of inner resistance in Li-ion batteries [10]. Eric et al. utilized capacity-based SOC measurements to compare the capacity and internal discharge resistance at various battery states of life [11]. Various research papers have introduced aging analysis using Electrochemical Impedance Spectrometry (EIS) technique, Saha et al. have analyzed shifts in EIS data (such as battery impedance) based on equivalent electric

Xiaowei Zhang is with the Department of Mechanical Engineering, McMaster University, Hamilton, Canada (e-mail: xiaowei\_zhang91@hotmail.com).

circuit parameters to predict the aging process [12]. Aging has been characterized in reduced-order electrochemical-based battery models, by tracking growth in the Solid Electrolyte Interface (SEI) layer in [13].

In this paper, an extensive battery aging test has been conducted over 12-months period on 5.4 Ah, 3.7 V Lithium polymer cells by using a set of real-world driving cycles. The experimental data for healthy (Capacity = 100%) and aged cells (Capacity = 80%) are used to fit the combined model based in an offline mode. Parameters of the combined model are tracked along various battery states of life. Finally, offline battery model parameters identification and state of charge estimation at various states of life have been implemented.

## II. AGING STUDY EXPERIMENT

As shown in Fig. 1, three benchmark driving cycles have been used during the aging study and model fitting; namely, an Urban Dynamometer Driving Schedule (UDDS), a light duty drive cycle for high speed and high load (US06), and a Highway Fuel Economy Test (HWFET) [14].

A mid-size all-EV model has been modified from an existing hybrid vehicle model and simulated in MATLAB/SimScape environment in order to generate the current profile from the velocity profile. The EV model consists of Li-ion battery pack, vehicle dynamic model, DC motor, DC-DC converter and vehicle speed controller. The aging test has been interrupted by a series of reference performance test schedules to track changes in the battery performance, these tests include:

- (1) A static capacity test at 1C, 2C, 3C, and 4C;
- (2) Static capacity test at low C-rate ( $C/15 - C/25$ ) in order to obtain the relationship between the open circuit voltage (OCV) and the state of charge (OCV-SOC);
- (3) A series of UDDS, US06, and HWFET driving cycles (*Schedule A*) (that scans the entire SOC range from 90% to approximately 20%);

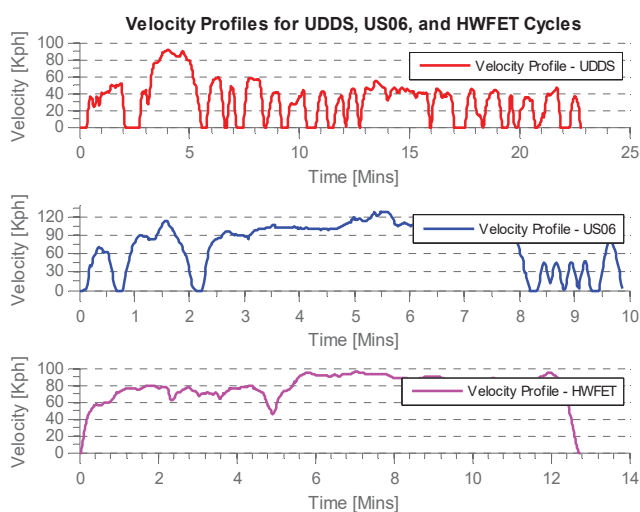


Fig. 1 Velocity profiles for the UDDS (upper), US06 (middle), and HWFET (lower) cycles [14]

The current generated from the electric vehicle has been converted from the pack level to the cell level based on the battery construction. Then the cell level current profile has been put into the experiment setup which includes 3 channel Arbin BT 2000 tester, 3 environmental chambers, AVL Lynx data acquisition system, AVL Lynx user-interface software and Li-ion cells to extract the terminal voltage and actual (reference) SOC. Driving *Schedule A* lasts approximately 290 minutes and is mixed by UDDS, US06, and HWFET test schedules. The current range of Schedule A is from -2C to 2C and covers the entire SOC from 90% to 20%. In order to demonstrate the difference in terminal voltage and SOC using the same driving schedule at different states of life, both voltage and SOC data for fresh (healthy) and aged battery at approximately 80% capacity for driving *Schedule A* are plotted as shown in Figs. 2 and 3, respectively.

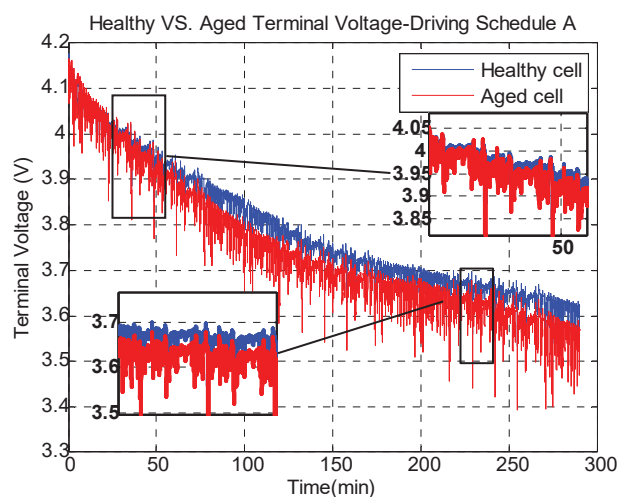


Fig. 2 Terminal Voltage for healthy cell and aged cell at 80% capacity - Driving Schedule A

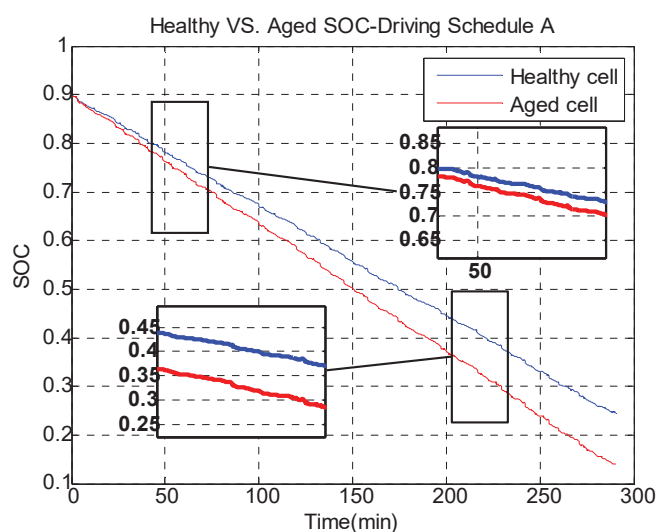


Fig. 3 SOC for healthy cell and aged cell at 80% capacity - Driving Schedule A

### III.OFFLINE PARAMETER IDENTIFICATION

Behavioral battery models use various empirical functions and formulas to describe the behavior of the battery cells. These models are simple to implement with fewer parameters to tune and are therefore easy to be implemented in real-time applications on a BMS. Examples are as follows [15].

- Shepherd model:  $y_k = E_0 - Ri_k - K_i/z_k$
- Unnewehr universal model:  $y_k = E_0 - Ri_k - K_i z_k$
- Nernst model:  $y_k = E_0 - Ri_k - K_2 \ln z_k + K_3 \ln(1 - z_k)$

In these models,  $y_k$  is cell terminal voltage (Replaced by  $V(t)$  in the following),  $i_k$  is input current,  $z_k$  is SOC,  $R$  is internal resistance which may change when charging and discharging,  $K_i$  is the polarization resistance chosen to make the model fit the data well. The combined model is defined as the collection of the three aforementioned models as [15]:

$$y_k = K_0 - Ri_k - \frac{K_1}{z_k} - K_2 z_k + K_3 \ln(z_k) + K_4 \ln(1 - z_k) \quad (1)$$

$$z_{k+1} = z_k - \left(\frac{\eta_i \Delta t}{C}\right) i_k \quad (2)$$

The combined model has been used in this paper since it is relatively simple and can provide an acceptable accuracy. The parameter vector  $\vec{\theta}$  consists of  $K_0, K_1, K_2, K_3, K_4, R_{charging}, R_{discharging}$  need to be estimated. The objective function is a cumulative sum of the squared voltage error as [16]:

$$\min_{\vec{\theta}} \int_0^T (V(t) - \hat{V}(t; \vec{\theta}))^2 dt \quad (3)$$

The objective function is targeted at minimizing the error between the model output terminal voltage  $\hat{V}(t)$  and the experimentally measured terminal voltage  $V(t)$ . The initial value, lower bound, and upper bound of the combined model parameters are presented in Table I.

	Initial value	Lower bound	Upper bound
R_charging	0.0177	0	0.1
R_discharging	0.0221	0	0.1
K0	3.5190	3	4.5
K1	0.0233	0	0.2
K2	0.0212	0	0.2
K3	-0.0867	-0.2	0.2
K4	-0.2950	-0.5	0.1

### IV.OPTIMIZED RESULTS

In this section, the offline parameter identification using Genetic Algorithm optimization is presented. Two states of life are considered; namely: fresh (healthy) battery state and aged (80% capacity). The GA algorithm has been applied to estimate battery parameters by using current and voltage data from *Schedule A* driving cycle. The model is simulated once

for every member of the population and the terminal voltage is further compared with the experimental terminal voltage. The GA optimization has been set to five runs and to 2500 population size. The algorithm has been conducted on a mobile workstation with 2.40 GHz, Dual-core i7-5500U processor.

The optimized terminal voltage vs. the actual (measured) voltage for both fresh and aged states are as shown below in Figs. 4 and 5, respectively. It is important to note that in this method, one set of parameters are used over the entire SOC range.

The optimized parameters for both healthy and aged cells are as shown below in Table II. The charging and discharging internal resistances:  $R_{charging}, R_{discharging}$  increase over the lifespan of the battery which reflects aging effects.

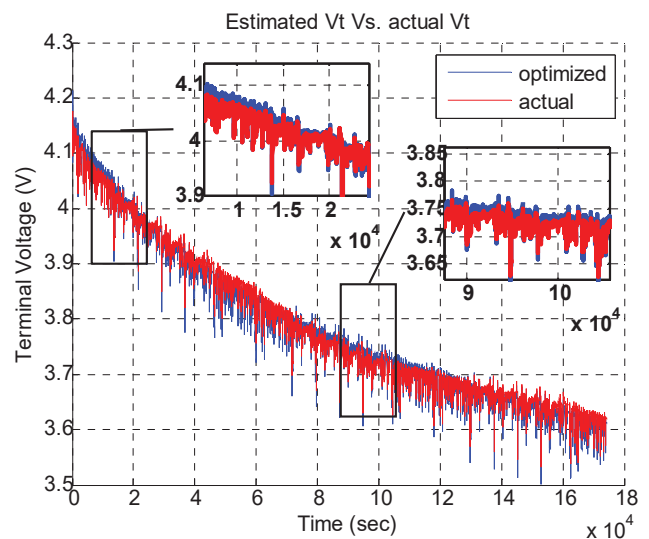


Fig. 4 Estimated Vs. actual terminal voltage for driving Schedule A (Healthy cell)

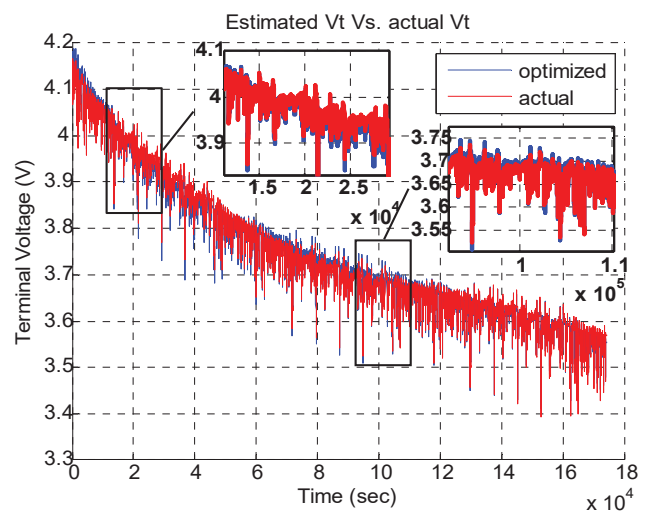


Fig. 5 Estimated Vs. actual terminal voltage for driving Schedule A (Aged cell)

### V.STATE-OF-CHARGE ESTIMATION

In this section, two estimation strategies have been applied to the battery to extract information regarding the battery SOC based on the optimized model. The strategies are known as EKF and SVSF, which both work in a predictive-corrective form.

TABLE II  
 OPTIMIZED PARAMETERS

	Healthy cell	Aged cell
R_charging	0.0130	0.0177
R_discharging	0.0103	0.0165
K0	3.5190	3.5190
K1	0.0233	0.0233
K2	0.0212	0.0876
K3	-0.0666	-0.0867
K4	-0.2950	-0.3282

Kalman Filter (KF) is the optimal filter on the conditions of the linear system and white noise. EKF is an extended form of KF and used for the non-linear system [17]. In the EKF, the system model is linearized around the current a priori state estimate and the linearized model is then used for calculating the Kalman gain to correct the predicted result.

The SVSF use the same concept as sliding mode control's switching action to correct state estimates and has been demonstrated robustness to modeling uncertainties and sensor noise [18]. It can be applied to linear or non-linear systems and for both state and parameter estimation applications. It works by using the SVSF gain that forces the states to switch back and forth across the state trajectory within a region referred to as the existence subspace which is a function of modeling uncertainties.

After trial and error, the system and measurement noise covariance in the EKF, and the convergence rate and boundary layers in the SVSF were obtained as in Table III.

The estimated SOC is initialized at 0.7, while the actual SOC is at 0.9. The SOC estimation results both for fresh cell and aged cell by EKF and SVSF are shown in Figs. 6 and 7. Fig. 8 shows the zoom-in configuration at the very beginning of the estimation process. Furthermore, the root mean square error (RMSE) associated with SOC estimation compared to the optimized model are shown in Table IV, respectively.

The result demonstrates that both EKF and SVSF provide fast convergence even though the error between the initial SOC and the actual SOC is quite different. Moreover, EKF and SVSF can provide a very good estimation accuracy if the filter parameters are properly tuned. Specifically, when the model is relatively accurate, such as aged cell model, EKF has shown better results compared to SVSF. However, as one can see in Table IV, the SOC error of optimized model of the aged cell is very small and is more accurate than the fresh cell. As the model uncertainties grow, SVSF can provide a better estimation result which shows a better robustness of SVSF compared to EKF.

TABLE III  
 THE EKF SYSTEM AND MEASUREMENT NOISE COVARIANCE, AND THE SVSF CONVERGENCE RATE AND BOUNDARY LAYERS

Filter Parameters	EKF	SVSF
Q	1e-10	/
R	0.1	/
$\psi$	/	3
$\Upsilon$	/	0.8

TABLE IV  
 ESTIMATION ERROR

RMSE	SOC error for Fresh Cell	SOC error for Aged Cell
EKF	2.26%	0.75%
SVSF	1.68%	1.30%
Optimized Model	6.83%	0.41%

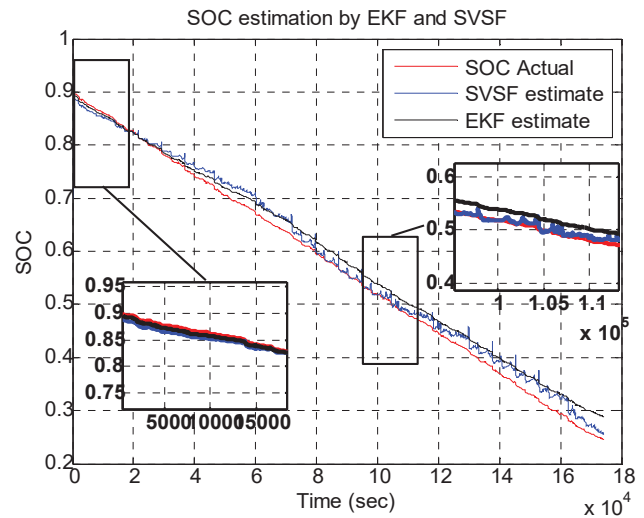


Fig. 6 Estimated Vs. Actual SOC by EKF and SVSF estimation strategies (Fresh cell)

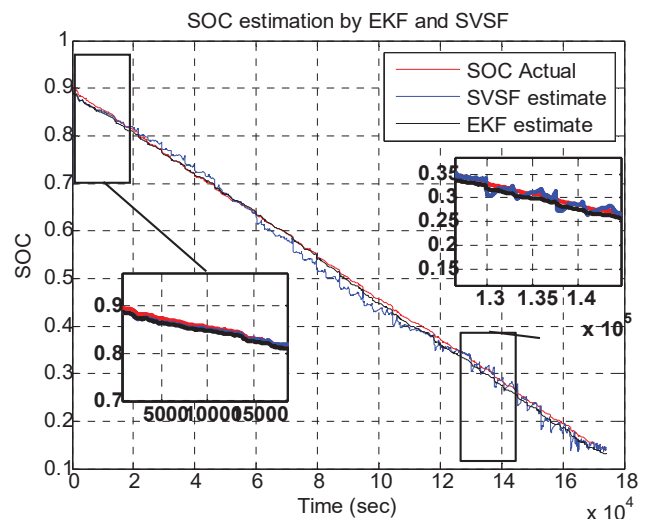


Fig. 7 Estimated Vs. Actual SOC by EKF and SVSF estimation strategies (Aged cell)

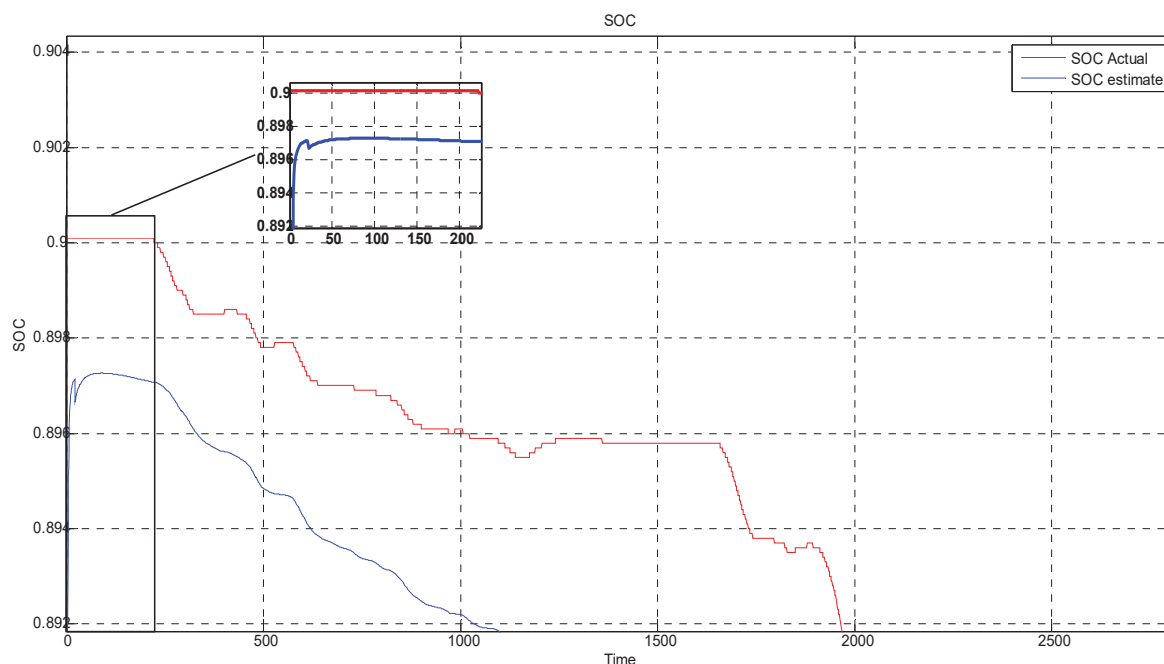


Fig. 8 Zoom-in at the very beginning of estimation process

#### VI. FUTURE WORK

Since EKF can provide a better result when the model is accurate but SVSF does well when there are much more model uncertainties. The future work will involve combining both strategies to improve the state-of-charge estimation accuracy and to estimate the state-of-health based on the optimized model over the entire battery lifespan.

#### VII. CONCLUSIONS

In this paper, an extensive battery aging study based on real-world driving scenarios has been conducted. The battery parameter based on the combined model has been identified in an offline mode. Model parameters, such as the internal resistance, change over the entire lifespan of the battery. Therefore, the BMS has to be adaptive to accommodate for the change in the battery physical parameters to ensure accurate SOC and SOH estimation. EKF and a relatively new state estimation strategy known as SVSF have been applied to estimate the battery state-of-charge and compared in terms of accuracy and robustness.

#### ACKNOWLEDGMENT

This research was facilitated through the MECH ENG 739 course: "Management and Control of Electric Vehicle batteries" offered by Dr. Ryan Ahmed at the faculty of Engineering, McMaster University.

#### REFERENCES

[1] S. Campanari, G. Manzolini, and F. Garcia de la Iglesia, "Energy analysis of electric vehicles using batteries or fuel cells through well-to-wheel driving cycle simulations," *J. Power Sources*, vol. 186, no. 2, pp. 464–477, 2009.  
[2] G. L. Plett, "Extended Kalman filtering for battery management systems

of LiPB-based HEV battery packs Part 1. Background," *J. Power Sources*, vol. 134, no. 2, pp. 252–261, 2004.  
[3] D. Anderson, "An evaluation of current and future costs for lithium-ion batteries for use in electrified vehicle powertrains," *Chem. ....*, no. May, p. 48, 2009.  
[4] A. Andrea, *Battery Management Systems for Large Lithium-Ion Battery Packs*. 2010.  
[5] M. Conte, F. V. Conte, I. D. Bloom, K. Morita, T. Ikeya, and J. R. Belt, "Ageing testing procedures on lithium batteries in an international collaboration context," *World Electr. Veh. J.*, vol. 4, pp. 335–346, 2011.  
[6] R. Ahmed, J. Gazzarri, S. Onori, S. Habibi, R. Jackey, K. Rzemien, J. Tjong, and J. LeSage, "Model-Based Parameter Identification of Healthy and Aged Li-ion Batteries for Electric Vehicle Applications," *SAE Int. J. Altern. Powertrains*, vol. 4, no. 2, pp. 2015–01–0252, Apr. 2015.  
[7] J. Remmlinger, M. Buchholz, M. Meiler, P. Bernreuter, and K. Dietmayer, "State-of-health monitoring of lithium-ion batteries in electric vehicles by on-board internal resistance estimation," *J. Power Sources*, vol. 196, no. 12, pp. 5357–5363, 2011.  
[8] V. Pop, H. J. Bergveld, P. P. L. Regtien, J. H. G. Op het Veld, D. Danilov, and P. H. L. Notten, "Battery Aging and Its Influence on the Electromotive Force," *J. Electrochem. Soc.*, vol. 154, no. 8, p. A744, 2007.  
[9] C. Guenther, B. Schott, W. Hennings, P. Waldowski, and M. A. Danzer, "Model-based investigation of electric vehicle battery aging by means of vehicle-to-grid scenario simulations," *J. Power Sources*, vol. 239, pp. 604–610, 2013.  
[10] A. T. Stamps, C. E. Holland, R. E. White, and E. P. Gatzke, "Analysis of capacity fade in a lithium ion battery," *J. Power Sources*, vol. 150, no. December 2004, pp. 229–239, 2005.  
[11] E. Wood, M. Alexander, and T. H. Bradley, "Investigation of battery end-of-life conditions for plug-in hybrid electric vehicles," *J. Power Sources*, vol. 196, no. 11, pp. 5147–5154, 2011.  
[12] J. C. B. Saha, K. Goebel, S. Poll, "An integrated approach to battery health monitoring using Bayesian regression and state estimation," *Ieee*, no. November, pp. 646–653, 2007.  
[13] R. Ahmed, M. El Sayed, I. Arasaratnam, J. Tjong, and S. Habibi, "Reduced-Order Electrochemical Model Parameters Identification and SOC Estimation for Healthy and Aged Li-Ion Batteries. Part I: Parameterization Model Development for Healthy Batteries," *IEEE J. Emerg. Sel. Top. Power Electron.*, vol. 2, no. 3, pp. 659–677, 2014.  
[14] J. R. Belt, "Battery Test Manual For Plug-In Hybrid Electric Vehicles," Dec. 2010.  
[15] G. L. Plett, "Extended Kalman filtering for battery management systems

- of LiPB-based HEV battery packs: Part 2. Modeling and identification,” *J. Power Sources*, vol. 134, no. 2, pp. 262–276, 2004.
- [16] J. C. Forman, S. J. Moura, J. L. Stein, and H. K. Fathy, “Genetic identification and fisher identifiability analysis of the Doyle-Fuller-Newman model from experimental cycling of a LiFePO<sub>4</sub> cell,” *J. Power Sources*, vol. 210, pp. 263–275, 2012.
- [17] G. L. Plett, “Extended Kalman filtering for battery management systems of LiPB-based HEV battery packs Part 3. State and parameter estimation,” *J. Power Sources*, vol. 134, no. 2, pp. 277–292, 2004.
- [18] S. Habibi, “The Smooth Variable Structure Filter,” *Proc. IEEE*, vol. 95, no. 5, 2007.